Existence of the spin-glass state in amorphous Fe

M. Yu and Y. Kakehashi
Department of Physics, Hokkaido Institute of Technology, Maeda 7-15-4-1, Teine-ku, Sapporo 006, Japan
(Received 24 January 1994)

The volume dependence of magnetic properties in amorphous Fe has been calculated on the basis of the finite-temperature theory of amorphous metallic magnetism which self-consistently determines the distribution of local magnetic moments. The calculated magnetic phase diagram on the T-V plane and magnetization-vs-volume curve show the existence of the spin-glass state in a wide range of volume ($10.50\ \text{Å}^3 \lesssim V \lesssim 12.5\ \text{Å}^3$) after disappearance of ferromagnetism. The results verify our previous conclusion of the spin-glass state in amorphous Fe, which is expected from the experimental data of Fe-rich amorphous alloys containing early transition metals and rare-earth metals, but disagree with those obtained from the supercell approaches in the ground-state electronic structure calculations. It is shown that the nonlinear magnetic couplings between the nearest-neighbor Fe local moments and the local environment effects on the amplitude of Fe local moments via structural disorder lead to the spin-glass state in the weak magnetic region, while the volume expansion develops the ferromagnetic couplings and therefore the ferromagnetism.

I. INTRODUCTION

Magnetism of amorphous Fe has been much investigated since the spin glasses (SG's) were found in Fe-rich amorphous alloys beyond 90 at. % Fe.[1-5] Systematic investigations of Fe-rich amorphous alloys containing early transition metals (TM) and rare-earth metals[6] have shown that the SG transition temperatures T_g beyond 90 at.% Fe are approximately the same value of 110 K, irrespective of the second elements. The result strongly suggested that the SG behaviors are dominated by structural disorder instead of configurational disorder, therefore intrinsic properties of amorphous Fe. Kakehashi[7,8] proposed a finite-temperature theory of amorphous metallic magnetism on the basis of the functional integral method[9] for thermal spin fluctuations and the distribution function method[10] for local magnetic moments (LM's) with structural disorder, and explained the SG behaviors around amorphous Fe in terms of the nonlinear magnetic couplings between Fe LM's and the local environment effects (LEE's) on the amplitude of Fe LM's, which are characteristic of itinerant-electron SG. Subsequently, Yu, Kakehashi, and Tanaka[11] extended the theory to amorphous alloys and derived the magnetic phase diagram of amorphous Fe-Zr alloys showing the ferromagnet-SG transition with increasing Fe concentration.

Recent ground-state electron-structure calculations and new experimental investigations, however, have raised controversial questions to the existence of SG. Krey and co-workers[12,13] constructed theoretically the amorphous compound with 54 Fe atoms in a box under the periodic boundary condition using the molecular-dynamics method, and calculated the ground state of amorphous Fe on the basis of generalized Hartree-Fock approximation to a realistic tight-binding Hamiltonian, which is called supercell approach. They found that the SG state is slightly higher than the ferromagnetic state (F) in energy, but may be stabilized only when the transverse spin components are taken into account. Hafner and co-workers[14,15] performed the same type of calculations using the structure model with 64 Fe atoms per unit cell and the first-principles tight-binding linear-muffin-tin-orbital (LMTO) method. They did not obtain the SG state at any density; the ferromagnetism with Fe LM's antiparallel to magnetization appears around expected density of amorphous Fe ($\rho = 7.5\ \text{g/cm}^3$), but persists until very large density ($\rho = 9.5\ \text{g/cm}^3$), beyond which the F-paramagnet (P) transition occurs. Experimentally, Handschuh *et al.*[16] have recently investigated the magnetic properties of amorphous Fe in Y/Fe/Y layered structure. They reported no indication of SG properties but ferromagnetism in amorphous Fe film with thickness less than 2.2 nm, though the ground-state magnetization shows a strong thickness dependence, which was attributed to volume effect.[16]

In order to resolve the discrepancy among various theories and experiments mentioned above, one has to examine the volume dependence of magnetism and the degree of structural disorder in amorphous Fe, as well as various approximations involved in the theories. In this paper, we investigate the volume dependence of magnetism in amorphous Fe using our theory of amorphous metallic magnetism and discuss the existence of the SG state in amorphous Fe from our point of view.

In the following section, we will briefly review the finite-temperature theory of amorphous metallic magnetism. We will present, in Sec. III, our numerical results for the magnetization and SG order parameter vs volume curves, the distribution functions of LM at various volumes, and the magnetic phase diagram on T-V plane. These results show the existence of the SG state in a wide range of volume. We will explain the SG-F transition with volume change and discuss the discrepancy between our results and those obtained from supercell approaches at the ground-state.[13,15] A summary of our results will be

given in Sec. IV together with further discussions on the SG state in amorphous Fe.

II. THEORETICAL FRAMEWORK

In the theory of amorphous metallic magnetism, we start from the degenerate-band Hubbard model with Hund's-rule coupling, and adopt the functional integral method,[9] which describes the thermal spin fluctuations. The method transforms the interacting Hamiltonian into a one-electron Hamiltonian with time-dependent random exchange fields acting on each site. Within the static and molecular-field approximations,[17] the thermal average of LM's on the central site 0 is given by a classical average of fictitious exchange field variable ξ on the same site:[7,17]

$$\langle m_0 \rangle = \frac{\int d\xi\, \xi e^{-\beta\Psi(\xi)}}{\int d\xi\, e^{-\beta\Psi(\xi)}} , \tag{1}$$

$$\Psi(\xi) = E_0(\xi) + \sum_{j=1}^{z} \Phi_{0j}^{(a)}(\xi) - \sum_{j=1}^{z} \Phi_{0j}^{(e)}(\xi) \frac{\langle m_j \rangle}{x_j} , \tag{2}$$

where β is the inverse temperature and z is the number of atoms on the nearest-neighbor (NN) shell. The energy functional $\Psi(\xi)$ consists of the single-site energy $E_0(\xi)$, the atomic $\Phi_{0j}^{(a)}(\xi)$, and the exchange $\Phi_{0j}^{(e)}(\xi)$ pair energies between sites 0 and j. The energy $-\Phi_{0j}^{(e)}(\xi)$ in Eq. (2) is regarded as the magnetic energy gain of the central LM's (ξ) when the NN LM ($\langle m_j \rangle$) on site j with amplitude x_j ($x_j^2 = \int d\xi\, \xi^2 e^{-\beta E_j(\xi)} / \int d\xi\, e^{-\beta E_j(\xi)}$) points up. These energies are given by

$$E_0(\xi) = \int d\omega\, f(\omega) \frac{D}{\pi} \mathrm{Im} \sum_{\sigma} \ln(L_{0\sigma}^{-1} - \mathcal{L}_{\sigma}^{-1} + F_{00\sigma}^{-1}) - N w_0(\xi) + \frac{1}{4} \tilde{J} \xi^2 , \tag{3}$$

$$\begin{bmatrix} \Phi_{0j}^{(a)}(\xi) \\ \Phi_{0j}^{(e)}(\xi) \end{bmatrix} = \tfrac{1}{2} \sum_{\nu=\pm} \begin{bmatrix} 1 \\ -\nu \end{bmatrix} \Phi_{0j}(\xi, \nu x_j) , \tag{4}$$

$$\Phi_{0j}(\xi, \xi_j) = \int d\omega\, f(\omega) \frac{D}{\pi} \mathrm{Im} \sum_{\sigma} \ln[1 - F_{0j\sigma} F_{j0\sigma} \tilde{t}_{0\sigma}(\xi) \tilde{t}_{j\sigma}(\xi_j)] , \tag{5}$$

$$\tilde{t}_{j\sigma}(\xi_j) = \frac{L_{j\sigma}^{-1} - \mathcal{L}_{\sigma}^{-1}}{1 + (L_{j\sigma}^{-1} - \mathcal{L}_{\sigma}^{-1}) F_{jj\sigma}} . \tag{6}$$

Here $f(\omega)$ and D in Eqs. (3) and (5) are the Fermi distribution function and the number of orbital degeneracy. N and $\tilde{J}$ in Eq. (3) are the d electron number and the effective exchange-energy parameter, respectively. $w_j(\xi)$ denotes the charge potential on site j, which is determined by the charge neutrality condition.

The random potential for σ-spin electrons on site j consists of the atomic level $\epsilon_j - \mu$ measured from chemical potential μ, the charge potential $w_j(\xi)$, the exchange potential $\tilde{J}\xi\sigma/2$, and the term due to uniform magnetic field h in unit of $g_e\mu_B/2$. Therefore, the inverse locator in Eqs. (3) and (6) is given by

$$L_{j\sigma}^{-1} = \omega + i\delta - \epsilon_j + \mu - w_j(\xi) + \tfrac{1}{2}\tilde{J}\xi\sigma + h\sigma , \tag{7}$$

δ being an infinitesimal positive number. $\mathcal{L}_{\sigma}^{-1}$ in Eqs. (3) and (6) denotes the effective medium for the random potentials $\{L_{j\sigma}^{-1}\}$ outside the NN shell, and the single-site $\tilde{t}$ matrix given by Eq. (6) is related to the scattering potential $L_{j\sigma}^{-1} - \mathcal{L}_{\sigma}^{-1}$. The effective medium for the diagonal disorder is determined by the coherent potential approximation (CPA) equation:[17]

$$[\langle \tilde{t}_{j\sigma}(\xi) \rangle]_s = 0 . \tag{8}$$

Here $[\,]_s$ ($\langle\,\rangle$) denotes the structural (thermal) average. The off-diagonal disorder between the central and the NN sites via transfer integrals t_{ij} is taken into account directly, and that outside the NN shell is described by an effective self-energy $\mathcal{S}_{\sigma}$. Therefore the coherent Green's functions $F_{ij\sigma}$ in Eqs. (3), (5), and (6) are given by

$$F_{00\sigma} = \left[\mathcal{L}_{\sigma}^{-1} + \sum_{j=1}^{z} \frac{t_{j0}^2}{\mathcal{L}_{\sigma}^{-1} - \mathcal{S}_{\sigma}} \right]^{-1} , \tag{9}$$

$$F_{0j\sigma} = F_{j0\sigma} = \frac{t_{j0}}{\mathcal{L}_{\sigma}^{-1} - \mathcal{S}_{\sigma}} F_{00\sigma} . \tag{10}$$

The effective self-energy $\mathcal{S}_{\sigma}$ should be chosen so that the structural average of the central coherent Green's function is equal to the exact one:

$$[F_{00\sigma}]_s = F_{\sigma} = \int \frac{[\rho(\epsilon)]_s d\epsilon}{\mathcal{L}_{\sigma}^{-1} - \epsilon} , \tag{11}$$

assuming that the average density of states (DOS) $[\rho(\epsilon)]_s$ for noninteracting electrons is known.

Equation (1) shows that the central LM is determined by the random variables of surrounding LM $\{\langle m_j \rangle\}$ and the squares of transfer integrals $\{y_j = t_{ij}^2\}$. Introducing the distributions $g(m_j)$ for the surrounding LM $\{\langle m_j \rangle\}$ and probability $p_s(y_j)$ for the squares of transfer integrals $\{y_j\}$, we obtain the distribution of the central LM via Eq. (1), since it should be identical with surrounding ones:

$$g(M) = \int \delta(M - \langle m_0 \rangle) \prod_{j=1}^{z} [p_s(y_j) dy_j g(m_j) dm_j] . \tag{12}$$

The self-consistent equations for the average LM $[\langle m \rangle]_s$ and the SG order parameter $[\langle m \rangle^2]_s$ are obtained from Eq. (12) after decoupling approximation at the right-hand side, which is correct up to the second moment.

$$\begin{bmatrix}[\langle m\rangle]_s\\ [\langle m\rangle^2]_s\end{bmatrix}=\int\begin{bmatrix}M\\ M^2\end{bmatrix}g(M)dM=\sum_{n=0}^{z}\Gamma\left[n,z,\frac{1}{2}\right]\sum_{k=0}^{n}\sum_{l=0}^{z-n}\Gamma(k,n,q)\Gamma(l,z-n,q)\begin{bmatrix}\langle\xi\rangle(n,k,l)\\ \langle\xi\rangle^2(n,k,l)\end{bmatrix}, \tag{13}$$

$$\langle\xi\rangle(n,k,l)=\int d\xi\,\xi e^{-\beta\Psi(\xi,n,k,l)}\Big/\int d\xi\,e^{-\beta\Psi(\xi,n,k,l)}, \tag{14}$$

$$\Psi(\xi,n,k,l)=E_n(\xi)+n\Phi^{(a)}_{+n}(\xi)+(z-n)\Phi^{(a)}_{-n}(\xi)-[(2k-n)\Phi^{(e)}_{+n}(\xi)+(2l-z+n)\Phi^{(e)}_{-n}(\xi)]([\langle m\rangle^2]_s^{1/2}/x), \tag{15}$$

$$q=\frac{1}{2}\left[1+[\langle m\rangle]_s/[\langle m\rangle^2]_s^{1/2}\right]. \tag{16}$$

Here the subscripts n and $+(-)$ in Eq. (15) denote the number of contracted atoms on the NN shell and the contracted (stretched) pair, respectively.

In the present approximation, the atomic local environment is described by a contraction or a stretch of the NN pair by $[(\delta R)^2]_s^{1/2}$, R being the NN interatomic distance. The random spin configuration on the NN shell is given by the up and down fictitious spins with magnitude $[\langle m\rangle^2]_s^{1/2}$ and probability q pointing up. Therefore, the local environment is specified by the number n of contracted atoms, the number k of up spins on the n contracted atoms, and the number l of up spins on the $z-n$ stretched atoms. The probability for such configuration is given by $\Gamma(n,z,\frac{1}{2})\Gamma(k,n,q)\Gamma(l,z-n,q)$ with use of the binomial distribution function $\Gamma(k,n,q)=[n!/k!(n-k)!]q^k(1-q)^{n-k}$. It turns out that the total number of configuration of about $2^z\times 2^z\sim 10^7$ are self-consistently taken into account.

In the same way, Eqs. (8) and (11) for the effective mediums $\mathcal{L}_\sigma$ and $\mathcal{S}_\sigma$ are written as

$$\sum_{\nu=\pm}\frac{1}{2}\left[1+\nu\frac{[\langle\xi\rangle]_s}{[\langle\xi\rangle^2]_s^{1/2}}\right]\left\{L_\sigma^{-1}(\nu[\langle\xi\rangle^2]_s^{1/2})-\mathcal{L}_\sigma^{-1}+F_\sigma^{-1}\right\}^{-1}=F_\sigma, \tag{17}$$

$$\sum_{\nu=\pm}\frac{1}{2}\left\{\mathcal{L}_\sigma^{-1}-z[y]_s\left[1+\nu\frac{[(\delta y)^2]_s^{1/2}}{\sqrt{z}\,[y]_s}\right](\mathcal{L}_\sigma^{-1}-\mathcal{S}_\sigma)^{-1}\right\}^{-1}=F_\sigma. \tag{18}$$

Here

$$\begin{bmatrix}[\langle\xi\rangle]_s\\ [\langle\xi^2\rangle]_s\end{bmatrix}=\sum_{n=0}^{z}\Gamma\left[n,z,\frac{1}{2}\right]\sum_{k=0}^{n}\sum_{l=0}^{z-n}\Gamma(k,n,q)\Gamma(l,z-n,q)\begin{bmatrix}\langle\xi\rangle(n,k,l)\\ \langle\xi^2\rangle(n,k,l)\end{bmatrix}, \tag{19}$$

$$\langle\xi^m\rangle(n,k,l)=\int d\xi\,\xi^m e^{-\beta\Psi(\xi,n,k,l)}/\int d\xi\,e^{-\beta\Psi(\xi,n,k,l)}. \tag{20}$$

Note that the fluctuation $[(\delta y)^2]_s^{1/2}/[(y)]_s$ is connected to that of the NN interatomic distance via $[(\delta y)^2]_s^{1/2}/[(y)]_s=2\kappa[(\delta R)^2]_s^{1/2}/[(R)]_s$, since $t_{j0}\propto R^{-\kappa}$ ($\kappa=3.8$ for amorphous Fe, Refs. 18 and 19).

In summary, the ferromagnetism ($[\langle m\rangle]_s\neq 0$, $[\langle m\rangle^2]_s^{1/2}\neq 0$), the SG state ($[\langle m\rangle]_s=0$, $[\langle m\rangle^2]_s^{1/2}\neq 0$), and the paramagnetism ($[\langle m\rangle]_s=[\langle m\rangle^2]_s^{1/2}=0$) are determined self-consistently by solving Eqs. (13), (17), and (18) together with the charge neutrality condition for the charge potential $w_j(\xi)$

$$N=\int d\omega\,f(\omega)\frac{(-D)}{\pi}\mathrm{Im}\sum_\sigma[L_{j\sigma}^{-1}(\xi)-\mathcal{L}_\sigma^{-1}+F_{jj\sigma}^{-1}]^{-1}. \tag{21}$$

III. NUMERICAL RESULTS

To clarify the difference between our theory[7,8,11] and recent ground-state calculations[13,15] based on the local-spin-density (LSD) functional theory, we chose the input parameters obtained from the LSD calculations more faithfully in the present investigations. We adopted the input DOS $[\rho(\epsilon)]_s$ for amorphous Fe (see Fig. 1), which was calculated by Fujiwara[20] with use of the relaxed dense random packing of hard spheres model consisting of 1500 atoms and the tight-binding LMTO recursion method for electronic structure calculation. The input DOS was scaled by a band width $W\propto r^{-\kappa}$ when volume is changed. Here r denotes the Wigner-Seitz atomic radius. The average coordination number z was chosen to be 12 as in the previous calculations.[7,8] Two values are chosen for the d electron numbers N of amorphous Fe;

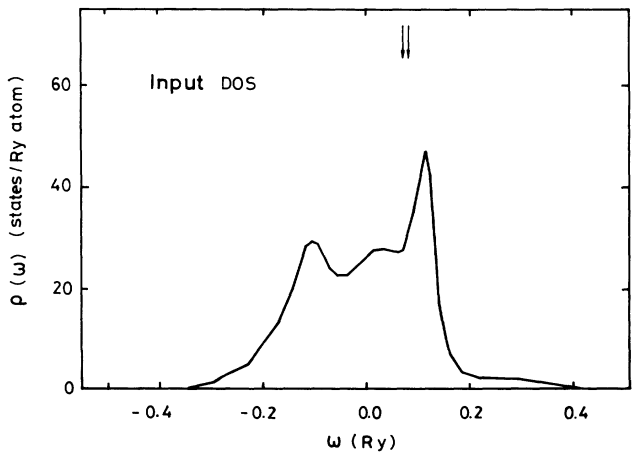

FIG. 1. Input DOS for amorphous Fe (Ref. 20) calculated with use of tight-binding LMTO recursion method. The arrows indicate the Fermi levels for $N=6.84$ (left) and 7.0 (right).

one is 6.84 calculated by Fujiwara[20] and the other is 7.0 used in our previous calculations.[7,8,11] The volume dependence of effective exchange-energy parameter $\tilde{J}$ was taken from the calculation by Andersen *et al.*[21] as follows:

$$\tilde{J}=\tilde{J}_0\left[-0.2\frac{r}{r_0}+1.2\right], \tag{22}$$

where $\tilde{J}_0=0.068$ Ry,[22] and $r_0=2.697$ a.u.[20] The fluctuation of interatomic distance $[(\delta R)^2]_s^{1/2}/[(R)]_s=0.06$ for amorphous Fe is estimated from the width of the first peak in experimental[23] and computer-generated[24] pair-distribution functions for amorphous Fe.

In Fig. 2, we present the volume dependence of calculated magnetization $[\langle m\rangle]_s$ (solid curves), SG order parameter $[\langle m\rangle^2]_s^{1/2}$ (dot-dashed curves), and amplitude of LM $[\langle m^2\rangle]_s^{1/2}$ (dotted curves) at 75 K. Obtained magnetizations for $N=6.84$ and 7.0 show a large value ($\geq 2.5\mu_B$) in the ferromagnetic region ($V\geq 13.0$ Å^3). With compression, the magnetization suddenly drops at the critical volume V^* (12.55 Å^3 for $N=7.0$, and 13.55 Å^3 for $N=6.84$), and the first-order transition from F to SG takes place, while the SG order parameter gradually decreases and below the volume $V\approx 10.50$ Å^3 the nonmagnetic state appears.

To explain the SG-F transition, we illustrate the exchange-pair energies in various local environments and the distribution of amplitude of Fe LM in Figs. 3 and 4. In weak magnetic region, for example around 11.5 Å^3 ($N=7.0$), the exchange-pair energies $-\Phi_{+n}^{(e)}(\xi,n)$ strongly depend on the number of contracted atoms n and show the nonlinear behaviors (i.e., the S-shaped curves) as shown in Fig. 3(a). This indicates that the central LM

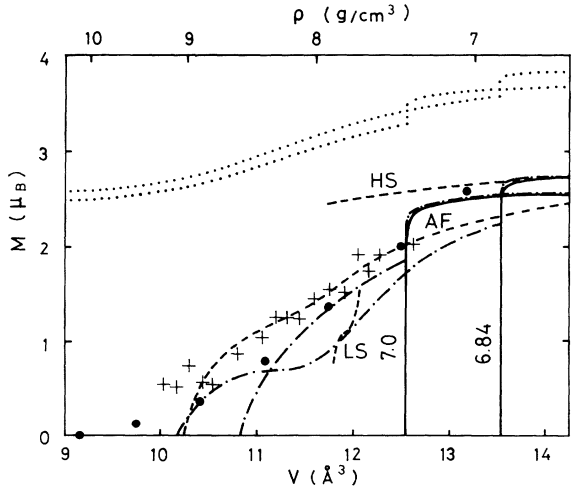

FIG. 2. Magnetization (solid curves), SG order parameter (dot-dashed curves), and amplitude of LM (dotted curves) vs volume curves for $N=6.84$ and 7.0 at 75 K. Calculated magnetizations for the high spin (HS), low spin (LS), and antiferromagnetic (AF) states of fcc Fe by Moruzzi, Marcus, and Kübler (Ref. 25) are presented by dashed curves, and those for amorphous Fe at the ground state by Krauss and Krey (Ref. 13) and Turek and Hafner (Ref. 15) are presented by crosses and full dots, respectively.

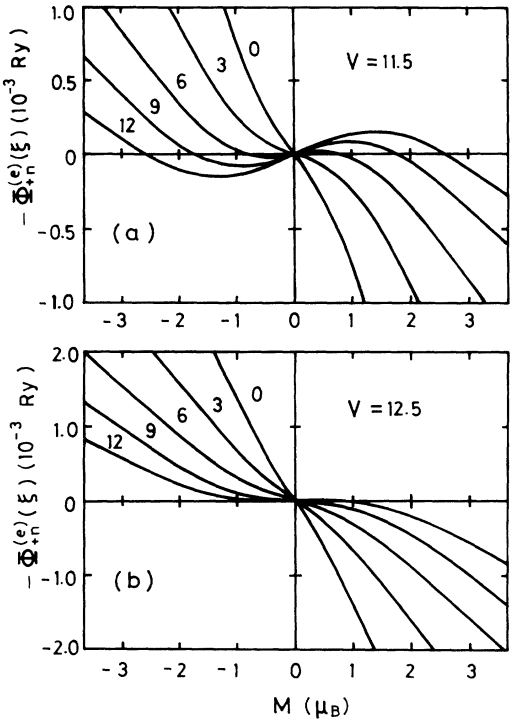

FIG. 3. Exchange pair energies $-\Phi_{+n}^{(e)}(\xi,n)$ in various local environments n at 11.5 Å^3 (a) and 12.5 Å^3 (b) for $N=7.0$ at 75 K. The numbers n of contracted atoms are shown by numerical in the figure.

with a large amplitude couples ferromagnetically with a neighboring LM, while the LM with a small amplitude antiferromagnetically couples with the neighboring LM. Since we have large amplitude fluctuations of LM (from $0.2\mu_B$ to $2.2\mu_B$) as shown in Fig. 4, the nonlinear couplings yield a competition between short-range ferromagnetic and antiferromagnetic interactions among the NN Fe LM's, therefore cause the SG state in this region. With expanding volume, the nonlinear behaviors of $-\Phi_{+n}^{(e)}(\xi,n)$ become weaker and tend to disappear near the SG-F phase boundary as shown in Fig. 3(b). In this

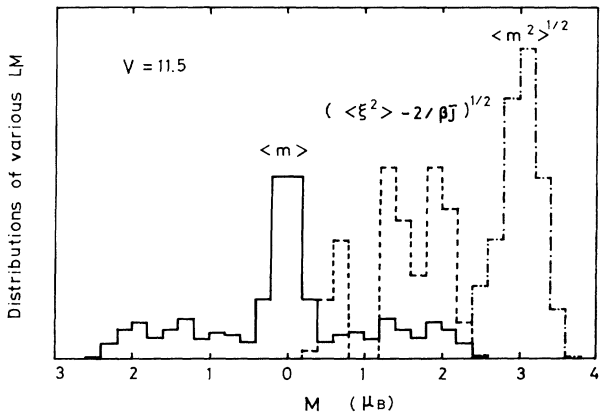

FIG. 4. Distributions of various LM: $\langle m\rangle$ (solid curve), $(\langle\xi^2\rangle-2/\beta\tilde{J})^{1/2}$ (dotted curve), and $\langle m^2\rangle^{1/2}$ (dashed curve) at 11.5 Å^3 for $N=7.0$ at 75 K.

region, the short-range ferromagnetic interactions become more favorable to form ferromagnetic clusters. Further expansion leads to the first-order transition to the ferromagnetic state.

Numerical results for fcc Fe calculated by Moruzzi, Marcus, and Kübler[25] (dashed curves) and those for amorphous Fe by Krauss and Krey[13] (crosses) and Turek and Hafner[15] (full dots) based on the supercell approach are also presented in Fig. 2. It is remarkable that the calculated SG order parameters show similar behavior to the magnetization curves in the high-spin (HS) state and the antiferromagnetic (AF) state in fcc Fe. This means that the amorphous and fcc Fe have approximately the same average magnitude of local magnetizations probably because both belong to the close-packed system.

A discrepancy is found between our results and those obtained from the supercell approach[13,15] at the ground-state (crosses and full dots) with decreasing volume. The former evidently shows the SG state below V^*, while in the latter the magnetization gradually deceases but remains finite until very small volume 9.75 Å^3 below that the system shows the paramagnetism. The supercell approach does not give the SG state at any volume though the average magnitude of local magnetizations is very similar to our results.

The same type of discrepancy is also found in the distributions of LM at various volumes. As an example, we present in Fig. 5, various distribution functions of LM for $N=7.0$ at 75 K together with the corresponding distributions by Turek and Hafner.[15] We found a good agreement between the two results in ferromagnetic region ($V > 12.55$ Å^3) showing a very narrow peak at large positive moment and a few negative moments with decreasing volume. However, in the SG region, our results show a very broad and symmetric distribution of SG behavior, while Turek's results show the asymmetric behavior leading to a net magnetization as plotted by the full dots in Fig. 2.

As we have discussed in our recent paper,[11] the discrepancy may be related to the small number of atoms accounted in the unit cell (64 atoms) and the periodic boundary condition for magnetic structure adopted in the supercell approaches. In general, 64 atomic configurations are enough to describe the electronic structure of nonmagnetic amorphous Fe, but not enough to describe a reasonable SG-F phase transition, since it is based on the competing interactions, which are sensitive to the atomic configuration. The periodic boundary condition for magnetic structure with the same unit cell as the crystalline one may be suitable to describe the strong ferromagnetism with no antiferromagnetic interactions, but may overestimate magnetization when there exists a strong competition between ferromagnetic and antiferromagnetic interactions because such competition generally leads to the magnetic structure with a unit cell larger than the crystalline one. In fact, the supercell approaches[13,15,26,27] did not explain the SG-F transition either in amorphous Fe-Zr (Ref. 6) or in substitutional Fe-Ni (Ref. 28) alloys. It is noteworthy that our theory self-consistently takes into account a large number of NN configuration ($\sim 10^7$), and explains the magnetic phase diagram in both amorphous Fe-Zr (Ref. 11) and substitional Fe-Ni (Ref. 29) alloys.

From the magnetization and inverse spin susceptibility vs temperature curves, we obtained magnetic phase diagram on T-V plane shown in Fig. 6. The transition from F to SG is of first order for the present choice of parameters. In this case, the self-consistent Eq. (13) determines the lower limit of the critical volume of ferromagnetic instability, which is plotted by dashed curves in Fig. 6. It is evident from the figure that the SG state appears in a

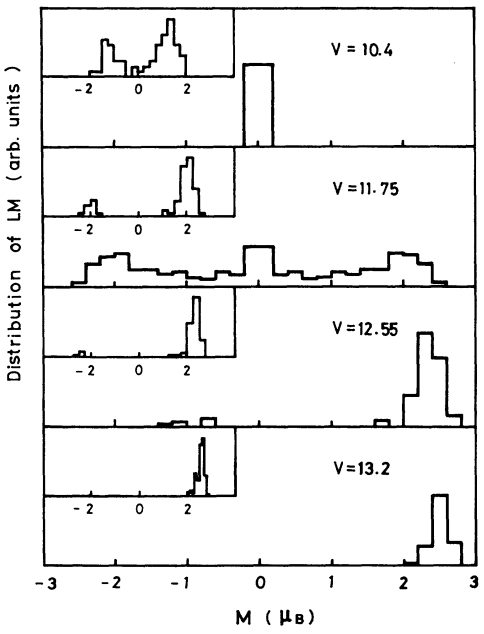

FIG. 5. Distributions of LM at various volumes for $N=7.0$ at 75 K. The results at the ground state with use of the supercell approach (Ref. 15) are also presented in the insets for the volumes: 13.19, 12.50, 11.75 and 10.42 Å^3 from the bottom to the top.

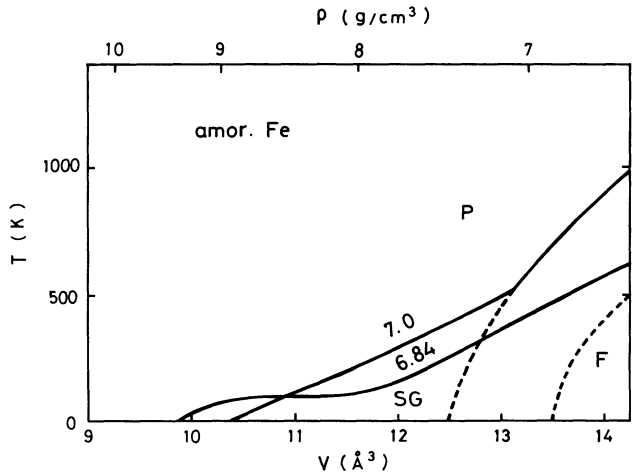

FIG. 6. Magnetic phase diagram on T-V plane for $N=6.84$ and 7.0 showing the F-SG-P transition with compression. The dashed curves show the lower volume limit of the phase boundary for the first-order transition.

wide range of volume, though the phase boundary considerably depends on a choice of parameters $\tilde{J}$ and N. Obtained SG transition temperatures T_g are between 230 and 360 K around 12.38 Å^3 [correspondingly roughly to that of sputter-deposited amorphous Fe (Ref. 15)], comparable with that expected from the experimental data of Fe-rich amorphous alloys ($\sim$110 K),[6] taking into consideration an overestimate of T_g by a factor of 2 in our calculation due to the molecular-field type of approximation.

IV. SUMMARY AND DISCUSSION

In this presentation, we have investigated the volume dependence of magnetism in amorphous Fe on the basis of our finite-temperature theory of amorphous metallic magnetism. Obtained magnetic phase diagram on T-V plane and magnetization vs volume curve show the F-SG-P transition with decreasing volume. In particular, they exhibit the SG state around reasonable volume of amorphous Fe, consistent with those expected from the experimental phase diagram of Fe-rich amorphous alloys containing early TM or rare-earth metals.[6] The SG state around amorphous Fe is caused by the nonlinear magnetic coupling between Fe LM's and the LEE's on the amplitude of LM's via structural disorder that are characteristic of itinerant magnetism.

We have attributed the discrepancy between our results and those based on the supercell approach at the ground state[13,15] to too small a number of atoms in a unit cell and the periodic boundary condition adopted in the supercell approaches.

We emphasize that the present results do not contradict with the recent data of amorphous Y/Fe/Y layered structure[16] showing the ferromagnetism. As we show in Fig. 7, the experimental data of magnetization are very sensitive to the thickness of Fe layer. If we extrapolate them linearly, the magnetization vanishes beyond 4.9 nm, suggesting the SG state in bulk amorphous Fe. Among various possibilities, Handschuh *et al.*[16] interpreted the strong dependence of magnetization on thickness in terms of volume effect; the average Fe-Fe distance near interface may be stretched by large Y atoms as the thickness of Fe layer is reduced.

Although we have concentrated on the volume dependence of magnetism in amorphous Fe in the present paper, it is also important that the magnetism strongly depends on the degree of structural disorder. The difference between the SG behavior in Fe-rich amorphous alloys containing early TM and the ferromagnetism in Fe-B amorphous alloys[30–32] beyond 9 at.% Fe may be attributed to this problem. It is highly desired to investigate the influence of the degree of structural disorder constructing a theory that interpolates between crystals and amorphous metals and alloys.

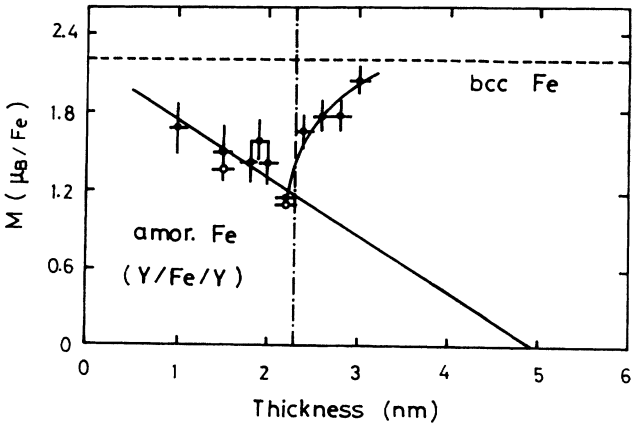

FIG. 7. Experimental data for average magnetic moment per Fe atom as a function of the Fe film thickness in Y/Fe/Y layered structure at 4.5 K (Ref. 16). The straight line shows an extrapolation of the data. The dot-dashed line shows the critical thickness above that a rapid transformation to a nanocrystalline structure throughout the total Fe film occurs. The dashed line indicates the value in bcc Fe. The open circles at 1.5 and 2.2 nm were determined by an especially careful correction of substrates contributions.

Further improvements of the present theory are also indispensable to verify the results presented here. For example, transverse components of LM, which were neglected in the present theory are considered to describe the transverse spin freezing according to the localized models.[33,34] Moreover, we only took into account the self-consistency of local magnetic moments $\langle m_j \rangle$ and neglected that of amplitudes $\langle m_j^2 \rangle$ in the present calculations. Since the amplitude fluctuations play an important role in the formation of the SG state in amorphous Fe, we have to examine the effects of amplitude fluctuations on the NN shell more seriously. We hope that these theoretical improvements and investigations will bring us more solid conclusion on the SG state in amorphous Fe.

ACKNOWLEDGMENT

This work was partly supported by the Grant-in-Aid for Scientific Research from the Ministry of Education, Science, and Culture in Japan.

[1]H. Hiroyoshi and K. Fukamichi, Phys. Lett. A **85**, 242 (1981); J. Appl. Phys. **53**, 2226 (1982).

[2]N. Saito, H. Hiroyoshi, K. Fukamichi, and Y. Nakagawa, J. Phys. F **16**, 911 (1986).

[3]H. Wakabayashi, K. Fukamichi, H. Komatsu, T. Goto, and K. Kuroda, in *Proceedings of the International Symposium on Physics of Magnetic Materials, Warsaw, 1986,* edited by W. Gorkowski, H. K. Lachowicz, and H. Szymczak (World Scientific, Singapore, 1987), p. 342.

[4]N. Karpe, K. V. Rao, B. Torp, and J. Bottiger, *Magnetic Properties of Amorphous Metals,* edited by A. Hernando, V. Madurga, M. C. Sanchez-Trujillo, and M. Vazquez (Elsevier,

Amsterdam, 1987), p. 340.
[5]D. H. Ryan, J. M. D. Coey, E. Batalla, Z. Altounian, and J. O. Ström-Olsen, Phys. Rev. B **35**, 8630 (1987); J. M. D. Coey, D. H. Ryan, and Yu Boliang, J. Appl. Phys. **55**, 1800 (1984); J. M. D. Corey and D. H. Ryan, IEEE Trans. Mag. MAG-20, 1278 (1984).
[6]K. Fukamichi, T. Goto, H. Komatsu, and H. Wakabayashi, in *Proceedings of the Fourth International Conference on the Physics of Magnetic Materials, Warsaw, 1988,* edited by W. Gorkowski, H. K. Lachowicz, and H. Szymczak (World Scientific, Singapore, 1989), p. 354.
[7]Y. Kakehashi, Phys. Rev. B **40**, 11 063 (1989); **41**, 9207 (1990).
[8]Y. Kakehashi, Phys. Rev. B **43**, 10 820 (1991); **47**, 3185 (1993).
[9]M. Cryot, J. Phys. (Paris) **33**, 25 (1972); J. Hubbard, Phys. Rev. B **19**, 2626 (1979); **20**, 4584 (1979); **23**, 5974 (1981); H. Hasegawa, J. Phys. Soc. Jpn. **46**, 1504 (1979); **49**, 178 (1980).
[10]F. Matsubara, Prog. Theor. Phys. **52**, 1124 (1974); S. Katsura, S. Fujiki, and S. Inawashiro, J. Phys. C **12**, 2839 (1979).
[11]M. Yu, Y. Kakehashi, and H. Tanaka, Phys. Rev. B **49**, 352 (1994).
[12]U. Krey, S. Krompiewski, and U. Krauss, J. Magn. Magn. Mater. **86**, 85 (1990); U. Krey, U. Krauss, and K. Krompiewski, *ibid.* **114**, 337 (1992).
[13]U. Krauss and U. Krey, J. Magn. Magn. Mater **98**, L1 (1991).
[14]Ch. Hausleitner and J. Hafner, Phys. Rev. B **42**, 5863 (1990); **45**, 115 (1992); **45**, 128 (1992).
[15]I. Turek and J. Hafner, Phys. Rev. B **46**, 247 (1992).
[16]S. Handschuh, J. Landes, U. Köbler, Ch. Sauer, G. Kisters, A. Fuss, and W. Zinn, J. Magn. Magn. Mater. **119**, 254 (1993).
[17]S. Q. Wang, W. E. Evenson and J. R. Schrieffer, Phys. Rev. Lett. **23**, 92 (1969); W. E. Evenson, J. R. Schrieffer, and S. Q. Wang, J. Appl. Phys. **41**, 1199 (1970).
[18]V. Heine, Phys. Rev. **153**, 673 (1967).
[19]U. K. Poulsen, J. Kollár, and O. K. Andersen, J. Phys. F **6**, L241 (1976).
[20]T. Fujiwara, Nippon Butsuri Gakkaishi **40**, 209 (1985).
[21]O. K. Andersen, J. Madsen, U. K. Poulsen, O. Jepsen, and J. Kollár, Physica **86-88B**, 249 (1977).
[22]J. F. Janak, Phys. Rev. B **16**, 255 (1977).
[23]M. Matsuura, J. Wakabayashi, T. Goto, H. Komatsu, and K. Fukamichi, J. Phys: Condens. Matter **1**, 2077 (1989).
[24]R. Yamamoto and M. Doyama, J. Phys. F **9**, 617 (1979).
[25]V. L. Moruzzi, P. M. Marcus, and J. Kübler, Phys. Rev. B **39**, 6957 (1989).
[26]H. Früchtl and U. Krey, J. Magn. Magn. Mater. **94**, L20 (1991).
[27]I. Turek, Ch. Becker, and J. Hafner, J. Phys. Condens. Matter **4**, 7257 (1992).
[28]T. Miyazaki, Y. Ando, and M. Takahashi, J. Magn. Magn. Mater. **60**, 219 (1984); **40**, 227 (1986); S. Ishio, K. Nushiro, and M. Takahashi, J. Phys. F **16**, 1093 (1986).
[29]Y. Kakehashi, Phys. Rev. B **38**, 474 (1988).
[30]N. Cowlam and G. E. Carr, J. Phys. F **15**, 1109 (1985); R. Hasegawa and R. Ray, J. Appl. Phys. **49**, 4174 (1978).
[31]C. L. Chien, D. Musser, E. M. Gyorgy, R. C. Sherwood, H. S. Chen, F. E. Luborsky, and J. L. Walter, Phys. Rev. B **20**, 283 (1979); C. L. Chien and K. M. Unruh, Phys. Rev. B **24**, 1556 (1981); C. L. Chien and K. M. Unruh, Nucl. Instrum. Math. **199**, 193 (1982).
[32]K. H. J. Bushcow and P. G. van Engen, J. Appl. Phys. **52**, 3557 (1981).
[33]M. Gabay and G. Toulouse, Phys. Rev. Lett. **47**, 201 (1981).
[34]J. R. Thomson, H. Guo, D. H. Ryan, M. J. Zuckermann, and M. Grant, Phys. Rev. B **45**, 3129 (1992); H. Ren and D. H. Ryan, *ibid.* **47**, 7919 (1993).